

This document is confidential and is proprietary to the American Chemical Society and its authors. Do not copy or disclose without written permission. If you have received this item in error, notify the sender and delete all copies.

QUANTITATIVE ANALYSIS OF TRANSFERRIN RECEPTOR 1 (TfR1) IN INDIVIDUAL BREAST CANCER CELLS BY MEANS OF LABELLED ANTIBODIES AND ELEMENTAL (ICP-MS) DETECTION.

Journal:	<i>Analytical Chemistry</i>
Manuscript ID	Draft
Manuscript Type:	Article
Date Submitted by the Author:	n/a
Complete List of Authors:	Montes-Bayon, Maria; Universidad de Oviedo, Physical and Analytical Chemistry Blanco-González, Elisa; Universidad de Oviedo, Physical and Analytical Chemistry Corte-Rodríguez, Mario; University of Oviedo, Department of Physical and Analytical Chemistry

SCHOLARONE™
Manuscripts

1
2
3 **QUANTITATIVE ANALYSIS OF TRANSFERRIN RECEPTOR 1 (TfR1) IN INDIVIDUAL BREAST**
4
5 **CANCER CELLS BY MEANS OF LABELLED ANTIBODIES AND ELEMENTAL (ICP-MS)**
6
7 **DETECTION.**
8
9

10
11 M. Corte-Rodríguez, E. Blanco-González, J. Bettmer and M. Montes-Bayón*

12
13 Department of Physical and Analytical Chemistry. Faculty of Chemistry. University of Oviedo.

14
15 Julián Clavería 8, 33006 Oviedo, Spain; Institute of Sanitary Research of Asturias (ISPA), Avenida
16
17 de Roma s/n, 33011 Oviedo, Spain.
18
19

20
21 * Correspondence to: montesmaria@uniovi.es
22
23
24
25
26

27 **ABSTRACT**
28
29

30 Cells are able to precisely control the amount of iron they acquire in the form of
31 transferrin (TF)-bound iron by modulating the synthesis of the transferrin receptor 1
32 (TfR1). In tumor cells, elevated TfR1 seems to be related to poorer outcome for patients.
33
34 Thus, the direct measurement of this biomarker in breast cancer tissues and cells might
35
36 serve as a prognosis biomarker. In this work, we have used Nd-labelled antibodies to tag
37
38 the TfR1 present on the cell surface of two cell models of breast cancer with different
39
40 malignancy (MCF7 and MDA-MB 231). For this aim, the monoclonal antibody anti-TfR1
41
42 is first labelled with a polymeric chelator (MAXPAR®) with subsequent incorporation of
43
44 several isotopic ^{143}Nd atoms. The characterization of the labelled antibody revealed a
45
46 stoichiometry of 20 Nd atoms per antibody molecule that can be used for further
47
48 quantification experiments. This antibody is used for cell tagging followed by single cell
49
50 analysis using inductively coupled plasma mass spectrometric (ICP-MS) detection. In this
51
52 case, cell introduction is conducted using a high efficiency nebulizer and spray chamber
53
54
55
56
57
58
59
60

1
2
3 to achieve transport efficiencies up to 55% for cells. Quantitative results revealed a
4
5 number of receptors per cell significantly higher in the case of the most malignant
6
7 phenotype (MDA-MB-231). Absolute and relative TfR1 concentration values are
8
9 obtained in individual cells for the first time using the proposed system.
10
11

12
13 **Key-words:** transferrin receptor 1, single cell analysis, ICP-MS, antibody labelling, breast
14
15 cancer.
16
17
18
19
20
21

22 **Introduction**

23
24
25 Iron is an essential element for cellular development. The main entrance mechanism of
26
27 Fe in cells occurs through its association to transferrin (Tf) that is further bound to
28
29 transferrin receptor 1 (TfR1) present in the cell surface. The Tf/TfR1 assembly is
30
31 internalized into the cell cytosol, rapidly matures and turns into a proton-pumping
32
33 endosome. The pH lowering in the endosome (pH close to 5.6 depending on cell type)
34
35 allows iron to be released from Tf and be either stored (into ferritin) or managed in the
36
37 different intracellular processes^{1, 2}. Iron-depleted Tf is then returned to the cell surface
38
39 where, encountering a pH of 7.4, the protein is released for another cycle of iron
40
41 transport. Therefore, TfR1 plays a critical role in iron homeostasis regulating this metal
42
43 uptake in the form of Fe₂-Tf complex. In this vein, fast proliferating cells with high iron
44
45 demand, such as cancer cells, constitutively express TfR1 at very high levels and can
46
47 further upregulate TfR1 expression in response to iron deficiency³. Recent publications
48
49 showed also that elevated TfR1 expression is related to poorer outcome for patients for
50
51 many types of cancer^{4, 5}. Thus, TfR1 can be considered as an important biomarker for
52
53 prognosis of some types of cancerous processes such as breast cancer since it affects
54
55
56
57
58
59
60

1
2
3 cell proliferation, migration, invasion and apoptosis^{6, 7}. But it can be also a suitable
4
5 biomarker for diagnosis and treatment of breast cancer patients at the early stage⁸.
6
7

8
9 Structurally, mammalian TfR1 comprises 760 residue subunits that can be divided into
10
11 three differential parts: a globular extracellular, a hydrophobic intramembranous and
12
13 cytoplasmic region⁹. Consisting of two monomers, TfR1 is linked by two disulfide
14
15 bridges, forming a 190 kDa molecule. The analysis of TfR1 in biological samples like cells
16
17 or tissues has been traditionally conducted by immunohistochemistry (IHC) which
18
19 provides qualitative or semiquantitative information¹⁰. As quantitative alternatives,
20
21 conventional enzyme-linked immunosorbent assays (ELISA) or reverse-phase protein
22
23 arrays (RPPA) have been applied to the determination of TfR1 and other iron
24
25 homeostasis biomarkers in biological fluids¹¹. As a major advantage, RPPA allows to
26
27 assess target protein expression quantitatively in large sample sets, while requiring only
28
29 a very low amount of biological sample making this platform attractive for the analysis
30
31 of clinical materials¹². However, in both cases, the applied samples are bio-fluids (serum,
32
33 plasma) or cell lysates. Therefore, these methods provide information of the total TfR1
34
35 concentration. This value corresponds to the fraction present on the cell membrane and
36
37 the fraction forming the Tf/TfR1 assembly within the cell cytosol after entering by
38
39 endocytosis.
40
41
42
43
44
45
46
47

48
49 In order to tackle chemical compositions and biological variations in individual cells,
50
51 strategies on single cell analysis have become increasingly important¹³. Among various
52
53 mass spectrometric techniques, single cell ICP-MS (SC-ICP-MS) allows the determination
54
55 of elemental compositions in individual cells since the first principal work has appeared
56
57 in 2005¹⁴. Nowadays, this technique has proven to be a versatile tool for studies on the
58
59
60

1
2
3 determination of constitutive elements¹⁵, the cellular uptake of metal-containing
4
5 drugs^{16, 17, 18}, and the incorporation of metallic nanoparticles¹⁹. In combination with
6
7 labelling strategies, further studies has shown the versatility of this technique to
8
9 characterize individual cells or bacteria^{20, 21}.

10
11
12
13 In this work, we have tried to develop an analytical strategy that permits the
14
15 quantification of TfR1 present uniquely in the cell membrane. Its concentration should
16
17 provide the most relevant information regarding the intracellular status upon iron
18
19 uptake and thus, the malignancy of a cell line or tissue. For this aim, we describe the
20
21 tagging of TfR1 present on the cell surface by means of lanthanide-labelled antibodies
22
23 in combination with the introduction of individual cells into the inductively coupled
24
25 plasma mass spectrometer (ICP-MS) ^{16, 22}.

26
27
28 For this aim, we have used the combination of a high-efficiency modified
29
30 microconcentric nebulizer with a spray chamber including a sheath argon flow for
31
32 maximum transport efficiency of the cells. The labelling of the antibody anti-TfR1 using
33
34 a polymeric chelator (MAXPAR[®]) with incorporated lanthanide ions serves as strategy
35
36 for cell tagging. The functionality of the labelled antibody is carefully assessed and the
37
38 number of incorporated lanthanides ions is determined. The developed methodology is
39
40 conducted using two breast cancer cell models of different malignancy, in which the
41
42 expression of TfR1 is expected to be different. The quantitative results are critically
43
44 compared with those obtained by commercial ELISA.
45
46
47
48
49
50
51
52
53

54 **MATERIALS AND METHODS**

55
56
57 **Reagents and materials.-** All solutions were prepared using 18 MΩ·cm⁻¹ de-ionized
58
59 water obtained from a Milli-Q system (Millipore, Bedford, MA, USA). Mouse anti-human
60

1
2
3 TfR1 monoclonal antibody was purchased from R&D Systems (Minneapolis, MN, USA).
4
5
6 Characterization of the antibody was conducted by size exclusion chromatography (SEC)
7
8 using 50 mmol L⁻¹ ammonium acetate pH 7.0 (Merck Millipore, Darmstadt, Germany) as
9
10 mobile phase at a flow rate of 0.7 mL min⁻¹ in a Superdex 200 10/300 GL column (300
11
12 mm x 100 mm i.d., GE Healthcare, Uppsala, Sweden). The column was previously
13
14 calibrated using protein standards (thyroglobulin 660 kDa, ferritin 450 kDa,
15
16 immunoglobulin G 150 kDa, albumin 66 kDa and alfa-lactalbumin 15 kDa) obtained from
17
18 Sigma-Aldrich (Madrid, Spain).
19
20
21
22

23
24 The antibody was labelled using a Maxpar X8 Antibody Labelling Kit (Fluidigm, San
25
26 Francisco, CA, USA), following the instructions of the manufacturer. For the reduction of
27
28 the antibody, tris(2-carboxyethyl)phosphine (TCEP) was purchased from Sigma-Aldrich.
29
30 For the purification steps, centrifugal filter units of 3 kDa and 50 kDa were used (Amicon
31
32 Ultra 0.5 mL, Merck Millipore). The purified conjugate was quantified by measuring the
33
34 absorbance at 280 nm using a NanoDrop 2000c (Thermo Fisher Scientific, Bremen,
35
36 Germany).
37
38
39
40

41
42 For cell fixation, a buffered aqueous solution of formaldehyde 4% (VWR Chemicals,
43
44 Pennsylvania, USA) was used as a fixative. Phosphate buffered saline (PBS), tris buffered
45
46 saline (TBS) and bovine serum albumin were obtained from Sigma Aldrich.
47
48

49
50 For single cell analysis, the transport efficiency was estimated using CyTOF[®] Calibration
51
52 Beads containing naturally abundant europium (Fluidigm). The transport efficiency of
53
54 liquid standards was calculated using the Reference Material 8012 of 30 nm gold
55
56 nanoparticles standard from NIST (Gaithersburg, MD, USA).
57
58
59
60

1
2
3 **Instrumentation.**- All ICP-MS experiments during this study were performed using the
4 triple quadrupole instrument iCAP TQ ICP-MS (Thermo Fisher Scientific, Bremen,
5 Germany) using the oxygen-TQ mode for the measurement of phosphorous (mass shift
6 from $^{31}\text{P}^+$ to $^{31}\text{P}^{16}\text{O}^+$ after reaction with oxygen in the reaction cell) and SQ-mode (single
7 quadrupole-mode) for $^{142}\text{Nd}^+$ and $^{153}\text{Eu}^+$ monitoring. For the single cell experiment, the
8 ICP-MS instrument was fitted with a high performance concentric nebulizer (HPCN) and
9 a small-volume on-axis spray chamber using a sheath gas flow (AIST, Tsukuba, Japan, see
10 Figure S1). A similar system has been described elsewhere²³. The cells were pumped
11 using a microflow syringe pump SP101i (Florida, USA) fitted with a 1 mL Hamilton syringe
12 (Nevada, USA) at $10\ \mu\text{L}\ \text{min}^{-1}$. The data were recorded in time-resolved analysis mode
13 during 3 min per analysis using a dwell time of 5 ms. Under these conditions, only a
14 single isotope could be measured in one run due to the sequential nature of the
15 measurements in a quadrupole system. The ICP-MS parameters are summarized in
16 Table S1.

17
18 For cell counting, a Flow Cytometer Cytoflex S Beckman Coulter (California, USA) was
19 used. The cell number was determined by absolute counting. For this aim, the peristaltic
20 pump of the flow cytometer was calibrated at $60\ \mu\text{L}\ \text{min}^{-1}$. Forward and scattered light
21 from the blue laser (488 nm) was registered in order to determine and count the intact
22 cells according to their size and morphology.

23
24 The characterization studies of the labelled antibody were carried out by SEC using an
25 HPLC system Agilent 1260 (Agilent Technologies, Tokyo, Japan). The column was a
26 Superdex 200 10/300 GL separation column (300 mm x 10 mm i.d., GE Healthcare Bio-
27 Sciences) having a fractionation range from 10 to 600 kDa. Detection was performed on-
28
29
30
31
32
33
34
35
36
37
38
39
40
41
42
43
44
45
46
47
48
49
50
51
52
53
54
55
56
57
58
59
60

1
2
3 line using both the integrated UV/VIS multiple wavelength detector and the iCAP TQ ICP-
4
5 MS.
6
7

8
9 **Cell cultures.**- Human breast cancer cell lines MCF7 and MDA-MB-231 were kindly
10 provided by J. M. Pérez Freije (Dept. of Biochemistry and Molecular Biology, University
11 of Oviedo). Cells were grown in T-25 flasks with Dulbecco's Modified Eagle Medium
12 (DMEM, LabClinics, Barcelona, Spain) and supplemented with 10% Fetal Bovine Serum
13 (Gibco, Life technologies, Madrid, Spain) and 5 $\mu\text{g mL}^{-1}$ Plasmocin prophylactic
14 (InvivoGen, Nucliber, Madrid, Spain) at 37°C in a 5% CO₂ atmosphere. Then, the cells
15 were washed with PBS (three times) and collected by trypsination.
16
17
18
19
20
21
22
23
24
25

26
27 **Analysis by commercial ELISA.**- Human TfR 1 was quantified by a commercial ELISA for
28 comparison using the Human Transferrin Receptor SimpleStep ELISA Kit from Abcam
29 (Cambridge, UK). This is a sandwich assay that uses an affinity tag-labelled capture
30 antibody and a reporter horseradish peroxidase (HRP)-conjugated detector antibody.
31
32 The capture of the analyte (TfR1) is performed in solution, and the entire complex is
33 then immobilized via immunoaffinity by an anti-tag antibody coating the well. Then, a
34 substrate solution (3,3',5,5'-tetramethylbenzidine, TMB) is added, which reacts with the
35 HRP to produce a blue coloration. The intensity of this signal is measured
36 spectrophotometrically at 450 nm and is proportional to the TfR 1 concentration.
37
38
39
40
41
42
43
44
45
46
47
48

49 For the ELISA, the cells were lysed using the Cell Extraction Buffer included in the kit.
50
51 The cell pellet was solubilized in the buffer, incubated on ice for 20 min and centrifuged
52 at 18,000 g for 20 min at 4°C.
53
54
55
56

57 **Cell fixation and tagging.**- After collecting the cells by trypsination, the cell number was
58 adjusted to 10⁶ cells per aliquot. The pellet was resuspended in 500 μL buffered
59
60

1
2
3 formaldehyde 4% and incubated for 15 min at room temperature to fix the cellular
4
5 structure during the labelling procedure. Afterwards, the cell pellet was washed with 3%
6
7 BSA in PBS by centrifugation for 5 min at 300 g and the pellet was resuspended in 200
8
9 μL of the antibody solution in 3% BSA in PBS. This suspension was incubated for 30 min
10
11 at room temperature and washed 3 times with 500 μL PBS (up to a total volume of 1500
12
13 μL) and 3 more times with 500 μL TBS (up to a total volume of 1500 μL) to minimize the
14
15 phosphorus background.
16
17
18
19
20

21 **Data treatment.**- For the data treatment of single cell suspension measurements, an
22
23 established iterative procedure was followed, based on averaging the entire data set
24
25 and collecting all data points that are three standard deviations (3σ) above the mean.
26
27 The resulting data set after removing the selected events is rearranged and the
28
29 procedure is repeated until no new data points are above the 3σ threshold. After the
30
31 selection of the single cell signals, those higher than 3σ above their mean were
32
33 discarded, as reported previously¹⁸, in order to eliminate multiple-cell events.
34
35
36
37
38

39 RESULTS AND DISCUSSION

40
41
42 **Studies on the antibody labelling reaction.**- The monoclonal antibody anti-TfR1 was
43
44 labelled using the sequential steps detailed in the MAXPAR[®] manufacturer's kit²⁴. To
45
46 conduct quantitative analysis of the number of receptors per cell it is necessary to
47
48 characterize the obtained product in terms of lanthanide ions per molecule of antibody.
49
50 This was conducted using complementary SEC-UV and SEC-ICP-MS. According to the
51
52 manufacturer's procedure, the first step involves the partial antibody reduction using
53
54 TCEP at 37°C for 30 min. The effectiveness of the reduction under these conditions can
55
56 be seen in the chromatogram of Figure 1A where the solid black trace corresponds to
57
58
59
60

1
2
3 the intact antibody and dotted trace to its reduced form. The unchanged retention time
4
5 after reduction (about 21 min) confirms the partial reduction of the antibody, with no
6
7 cleavage of the two antibody domains and, therefore, no change on its total molecular
8
9 mass. The high-intensity peak obtained at 26.5 min for the reduced antibody
10
11 corresponds to the EDTA present in the reduction buffer.
12
13
14

15
16 Figure 1A shows also a grey trace corresponding to the antibody after labelling. As can
17
18 be seen, there is a significant shift in the retention time towards shorter time, thus
19
20 higher molecular mass. According to the literature, the labelling polymer could contain
21
22 an average of 22 DTPA (diethylenetriaminepentaacetic acid) individual chelators that
23
24 could allocate up to 22 Nd ions providing a whole mass tag of approximately 23 kDa²²,
25
26
27
28
29
30
31
32
33
34
35
36
37
38
39
40
41
42
43
44
45
46
47
48
49
50
51
52
53
54
55
56
57
58
59
60
25. To confirm the presence of Nd in the labelled antibody, SEC-ICP-MS was also used. In
Figure 1B, it is possible to observe a maximum in the ¹⁴²Nd⁺ signal at about 16 min
matching the UV trace and ascribed to the labelled antibody. The second peak at about
20 min could correspond to the excess of unreacted polymeric tag. The combined
information of the UV and ICP-MS traces confirm that the antibody has been totally
labelled (no signal of unlabeled species can be seen) and a low carryover of unreacted
polymer. In any case, the unreacted polymeric tag will be further removed during the
washing steps of the labelling protocol.

To obtain the number of Nd ions labelling each antibody, the commercial heterogeneous
sandwich ELISA kit used for the determination of TfR1 was modified by changing the
detection antibody by 1 $\mu\text{g}\cdot\text{mL}^{-1}$ of the Nd-labelled antibody. The rest of the protocol
was maintained as recommended by the manufacturer. Three different antigen (TfR1)
concentrations were tested (0.01, 0.04 and 0.08 nmol L^{-1}). After the last wash, instead

1
2
3 of adding the TMB substrate for HRP detection in the commercial ELISA, 100 μL of 2%
4
5 HNO_3 were added to each well and incubated for 10 min at room temperature.
6
7
8 Neodymium in this solution was quantified by flow-injection analysis using ICP-MS
9
10 detection (FIA-ICP-MS). By applying adequate conversions, the area of each FIA peak can
11
12 be transformed into the absolute amount of Nd for each of the analyzed TfR1 standards.
13
14
15 In Figure 2, the correlation between the moles of Nd and those of TfR1 is depicted where
16
17 the slope of the adjusted curve provides the Nd:antibody stoichiometry²⁶. As can be
18
19 seen, the linear regression ($y=21.23 x + 0.44$, $R^2=0.9920$) provides a stoichiometry of
20
21 approximately 21 moles of neodymium per mole of anti-TfR1 antibody. This result is in
22
23 good agreement with the expected 22 DTPA chelator molecules in each Maxpar®
24
25 polymer tag, meaning that only one polymer molecule attaches to the antibody.
26
27
28
29
30

31 **Recognition capabilities of the Nd-labelled antibody in a modified ELISA.** - One of the
32
33 methods to quantitatively address the presence of TfR1 in biological fluids is an ELISA
34
35 assay. The selected one is based on a sandwich immune assay, including an anti-tag pre-
36
37 coated well plate where the affinity tag-labelled capture antibody is immobilized after
38
39 the sandwich formation with the HRP-labelled secondary antibody. This assay, which is
40
41 commercially available, allows the determination of TfR1 in liquid samples coming from
42
43 biological fluids or cell lysates. In the latter case, the method implies the cell lysis with
44
45 specific reagents (e.g. detergents) that permit to stabilize the TfR1 in solution before
46
47 measurement. The TfR1 concentration results provided in this case include the cell
48
49 surface as well as the internalized receptors.
50
51
52
53
54
55

56 To ensure that the recognition capabilities of the antibody are kept after the labelling
57
58 with the Nd-loaded polymer, a set of cell culture samples were analyzed using both, the
59
60

1
2
3 commercial ELISA with spectrophotometric detection and the ICP-MS based assay with
4
5 the Nd-labelled antibody. For this purpose, independent triplicates of each breast
6
7 cancer cell line (MDA-MB-231 and MCF7) were lysed as previously explained. After the
8
9 lysis, two aliquots of each sample were analyzed independently with the two assays. The
10
11 results of both sets analyses are shown in Table 1. As observed, the results are in good
12
13 agreement in both cell lines, with relative differences around 7-8.3% for the modified
14
15 ELISA with respect to the commercial assay. These values suggest the usefulness of the
16
17 Nd-labelled antibody and its stoichiometric characterization for further analysis.
18
19
20
21
22

23 Regarding the comparative values within the two cell lines analyzed, the MDA-MB-231
24
25 (most malignant and proliferating phenotype) shows a much higher number of
26
27 receptors than the MCF-7, in agreement with previously published work²⁷. However, the
28
29 bulk analysis reflects the concentration of the receptors that are present at the cell
30
31 surface but also inside the cell cytosol from previously endocytosed Tf/TfR1 assemblies.
32
33 The aim of the present work is the possibility to distinguish among both, to the best of
34
35 our knowledge never reported before, and with different biological implications than
36
37 the total TfR1 concentration.
38
39
40
41
42
43

44 **Determination of the sample introduction efficiency for single cell (SC)-ICP-MS.-** For
45
46 single cell analysis, a sample introduction set-up consisting on a high-performance
47
48 concentric nebulizer (HPCN) and a small-volume on-axis spray chamber utilizing a sheath
49
50 gas flow were used as described previously²³. In order to characterize the system and to
51
52 obtain the sample introduction efficiency, two different models were evaluated.
53
54 Europium-doped polystyrene beads of about 3 μm of diameter (lower diameter than
55
56 eukaryotic cells but higher density) and the same MDA-MB-231 human cells used for the
57
58
59
60

1
2
3 experiments. Whereas the calibration beads are a good and stable option for a daily
4
5 performance test, the use of the actual cells is preferred for the calculation of the
6
7 transport efficiency because the differences in size, density and general behavior during
8
9 the nebulization are avoided. The calibration beads were diluted to 33000 beads·mL⁻¹.
10
11 In the case of the cells, they were precisely counted by flow cytometry after labelling,
12
13 and the suspensions were adjusted to around 2.5·10⁵ cells·mL⁻¹. The suspensions were
14
15 sequentially measured by SC-ICP-MS monitoring ¹⁴²Nd and ³¹P for the cells and ¹⁵³Eu for
16
17 the beads. To obtain the transport efficiency, the expected events were compared with
18
19 the obtained events, according to a previous publication and using the statistical
20
21 restrictions previously detailed.¹⁸
22
23
24
25
26
27

28 Figure S2a shows histograms of the Eu-doped beads measured by ICP-TQ-MS and
29
30 applying 5 ms as dwell time. As can be seen, since these are manufactured beads, the
31
32 dispersion in the intensity of the events is very low, and the detection of multiple
33
34 particles in a single event can be considered negligible. By comparing the number events
35
36 detected and the expected ones it is possible to calculate a bead transport efficiency of
37
38 52%. Similarly, in the case of the cells, P was chosen as constitutive element to be
39
40 measured off-mass using the oxide formation (³¹P¹⁶O⁺ at m/z 47). Since these cells were
41
42 already labelled with the anti-TfR1 antibody, the Nd⁺ was also used for the same
43
44 purpose. The results observed for these cells can be seen in Figure S2b and S2c,
45
46 respectively. In this case, the results are due to the biological variety more dispersed
47
48 than in the case of the beads. More importantly, the transport efficiency calculated for
49
50 cells turned out to be very similar, 55% for P and 50% for the Nd label. These results
51
52 revealed that the antibody labelling on the cell surface was successful.
53
54
55
56
57
58
59
60

Analysis of TfR1 present at the cell surface by single cell ICP-MS in MDA-MB-231 and

MCF7 cells.- Tagging of breast cancer cells with the labelled antibody was conducted as described before, using formaldehyde for fixation. In order to ensure that enough labelled antibody was added to tag every receptor at the cell surface, three different antibody concentrations were added to three independent cell suspensions each containing 10^6 cells. It is expected that different antibody concentrations could affect the signal in two different ways: 1) increasing the height of the detected events if more TfR1 are tagged upon increasing the concentration of the antibody and 2) increasing the number of events since cells with lower number of TfR1 could be tagged and, therefore, visualized at higher antibody concentrations. The results are summarized in the boxplot of Figure 3. As can be seen, the height of the detected events increases when the cells are treated with $1 \mu\text{g}\cdot\text{mL}^{-1}$ antibody, but there is neither significant variation in the height of the events nor the number of detected events above this concentration. Therefore, the antibody concentration of $1 \mu\text{g}\cdot\text{mL}^{-1}$ seems to represent sufficient excess to tag all the TfR1 present in the cell surface of MDA-MB-231.

Then, this concentration was used to tag the two cell lines of breast cancer: MCF7 (less malignant) and MDA-MB-231 (more aggressive and proliferative phenotype). The type of detected events can be seen in Figure 5 where the signal for $^{142}\text{Nd}^+$ are plotted for the two cell lines. In this case, the phosphorous signal has been monitored as internal control to verify that the cell introduction system is working correctly and that the number of cell events is approximately constant among different days.

The first finding was that the lower height of the events detected for phosphorous (data not shown here) in the MCF7 agrees with the fact that this cell line

1
2
3 shows a different morphology and probably size than MDA-MB-231²⁸. Lower signal
4
5 intensities of $^{142}\text{Nd}^+$ in the events were observed for the MCF7 cell line in comparison to
6
7 MDA-MB-231. Although the analyzed suspensions contained the same number of cells,
8
9 this observation reflects a descent in the number of TfR1 as expected from the bulk
10
11 results obtained in the first part of the work (Table 1). To convert the height of the Nd
12
13 events into Nd mass per cell, a calibration curve was constructed using Nd standards. In
14
15 this case, the transport efficiency used for the calculations was 70% based on the
16
17 analysis of a 30 nm gold nanoparticles standard with the same system²⁹. The Nd mass in
18
19 each cell was then easily converted to the mass of antibody using the obtained
20
21 stoichiometry (20 Nd ions per antibody) and further, to the number of antigen molecules
22
23 (TfR1) per cell.
24
25
26
27
28
29

30
31 The boxplot of the results corresponding to three independent cell cultures can be seen
32
33 in Figure 5. Mean values of about $2.3 \cdot 10^4$ receptors per individual cell surface in the
34
35 MDA-MB-231 while only $6.4 \cdot 10^3$ receptors per individual cell surface in the MCF7 were
36
37 obtained. These results showed, consistently, that the number of TfR1 per cell is
38
39 different between cell lines being about 4-fold higher in the case of the most malignant
40
41 phenotype (MDA-MB-231).
42
43
44
45

46
47 Such finding confirms that fast proliferating cells, like MDA-MB-231 express TfR1 at very
48
49 high levels, and this expression can even increase in response to iron deficiency, which
50
51 is also sustained by previous measurements of intracellular Fe concentration in these
52
53 two models.³⁰ This shows the importance of the developed methodology that could be
54
55 further implemented for the absolute measurement of other malignancy biomarkers at
56
57
58
59
60

1
2
3 the single cell level with high sensitivity and minimum sample handling (no need for cell
4
5 lysis).

6
7
8 **Membrane and intracellular TfR1.**- The use of the Nd-labelled antibody permitted to
9
10 address the total TfR1 concentration present in the cell lysate, as shown in a previous
11
12 section, with comparably good results to the commercial ELISA (Table 1). Such results
13
14 can be converted in the number of TfR1 per cell by taking into account the precise
15
16 number of cells in each sample obtained by flow cytometry. In addition, the single cell
17
18 experiments allow the determination of the TfR1 per cell present at the cell membrane.
19
20 Thus, the difference between these two sets of values permits to illustrate the
21
22 intracellular level of TfR1.
23
24
25
26

27
28 These results are shown in Table 2 for three independent cell cultures of each of the cell
29
30 lines. As can be seen, the bulk data results reveal mean values of $2.3 \cdot 10^5$ receptors per
31
32 cell for MCF7 and $1.3 \cdot 10^6$ in the case of MDA-MB-231. Thus, the MDA-MB-231 shows, in
33
34 both cases, substantially higher TfR1 levels. These values are in the order of other
35
36 reported by using indirect methods like those based on the radioactive tagging of
37
38 transferrin and measuring the induced radioactivity of cells after formation of the
39
40 Tf/TfR1 assembly that is rapidly internalized (min)³¹. However, regarding the number of
41
42 receptors present at the cellular membrane, no information from the literature could
43
44 be obtained. Since an important research line focuses on the use of TfR1 as potential
45
46 entrance mechanism for viruses into cells³², this is an extremely valuable information.
47
48 Moreover, nanomedicine and antibodies targeting TfR1 (at the cell membrane) have
49
50 been developed for tumor-specific targeted therapy, in the field of precision oncology.³³
51
52 Thus, the obtained information reveals the extraordinary potential of the single cell
53
54
55
56
57
58
59
60

1
2
3 strategy to address, quantitatively, the expression of cell biomarkers present only on the
4
5 cell surface at extremely low concentration levels thanks to the excellent capabilities of
6
7 ICP-MS detection.
8
9

10 **Conclusions**

11
12
13
14 The use of labelled antibodies in combination with cell tagging and single cell analysis
15
16 via ICP-MS seems to be a promising approach for the determination of clinical
17
18 biomarkers, particularly present at the cell surface. For this aim, the MAXPAR® labelling
19
20 kit has proved to be successful for labelling the anti-TfR1 monoclonal antibody obtaining
21
22 a stoichiometry of approximately 20 Nd ions per antibody molecule that might correlate
23
24 with the presence of one chelating polymer attached to an antibody molecule. The
25
26 tagging of cells after fixation with this antibody showed throughout this work to occur
27
28 efficiently and in a reproducible way. Furthermore, the tagged cells are transported into
29
30 the ICP-MS through a high-efficiency nebulizer and spray chamber and can be detected
31
32 by P and Nd monitoring. The quantitative analysis of Nd in the obtained cell events can
33
34 be used for further evaluation of the number of TfR1 on the surface of different cell
35
36 cultures of breast cancer. The obtained results showed that the developed strategy
37
38 exhibits a great potential for the quantitative analysis of TfR1 at the single cell level
39
40 without sorting to cell disruption and minimum handling.
41
42
43
44
45
46
47
48
49
50
51
52
53
54
55
56
57
58
59
60

Acknowledgements

The authors would like to acknowledge the regional funding from the Government of Asturias through the Science, Technology and Innovation Plan (PCTI) co-financed by FEDER funds (Ref. FC-GRUPIN-IDI/2018/000242) and the funding from the Spanish Ministry of Economy, Industry and Competitiveness (MINECO) through the project CTQ2016-80069-C 2-1R, as well as the support from the Asturian Foundation for Biosanitary Research and Innovation (FINBA). Thermo Fisher Scientific, Bremen, Germany, and Teledyne Cetac Technologies, Omaha, NE, USA, are acknowledged for the instrumental support.

References

- ¹ B. Silva and P. Faustino. An overview of molecular basis of iron metabolism regulation and the associated pathologies. *Biochim. Biophys. Acta (BBA) - Molecular Basis of Disease*, 2015, 1852, 1347-1359.
- ² O. Kakhlon and Z.I. Cabantchik. The labile iron pool: characterization, measurement, and participation in cellular processes (1). *Free Radic. Biol. Med.*, 2002, 33:1037-1046-
- ³ X. Huang. Does iron have a role in breast cancer? *Lancet Oncol.*, 2008, 9:803-807.
- ⁴ Y. Shen, X. Li, D. Dong, B. Zhang, Y. Xue and P. Shang. Transferrin receptor 1 in cancer: a new sight for cancer therapy. *Am. J. Cancer Res.*, 2018, 8:916-931.
- ⁵ A. Calzolari, I. Oliviero, S. Deaglio, G. Mariani, M. Biffoni, N.M. Sposi, F. Malavasi, C. Peschle and U. Testa. Transferrin receptor 2 is frequently expressed in human cancer cell lines. *Blood Cells Mol. Dis.*, 2007, 39:82-91.
- ⁶ B. Wang, J. Zhang, F. Song, M. Tian, B. Shi, H. Jiang, W. Xu, H. Wang, M. Zhou, X. Pan, J. Gu, S. Yang, L. Jiang and Z. Li. EGFR regulates iron homeostasis to promote cancer growth through redistribution of transferrin receptor 1, *Cancer Lett.*, 2016, 381:331-340.
- ⁷ E. Ryschich, G. Huszty, H.P. Knaebel, M. Hartel, M.W. Buchler and J. Schmidt. Transferrin receptor is a marker of malignant phenotype in human pancreatic cancer and in neuroendocrine carcinoma of the pancreas. *Eur. J. Cancer*, 2004, 40:1418–1422.
- ⁸ G.Y. Lui, Z. Kovacevic, V. Richardson, A.M. Merlot, D.S. Kalinowski and D.R. Richardson. Targeting cancer by binding iron: Dissecting cellular signaling pathways, *Oncotarget*, 2015, 6:18748-18779.
- ⁹ E. Gammella, P. Buratti, G. Cairo and S. Recalcati. The transferrin receptor: the cellular iron gate. *Metallomics*, 2017, 9:1367-1375.
- ¹⁰ H.O. Habashy, D.G. Powe, C.M. Staka, E.A. Rakha, G. Ball, A.R. Green, M. Aleskandarany, E.C. Paish, R.D. Macmillan, R.I. Nicholson, I.O. Ellis and J.M.W. Gee. Transferrin receptor (CD71) is a marker of poor prognosis in breast cancer and can predict response to tamoxifen. *Breast Cancer Res. Treat.*, 2010, 119: 283–293.
- ¹¹ S. Pizzamiglio, M. De Bortoli, E. Taverna, M. Signore, S. Veneroni, W. Chi-shing Cho, R. Orlandi, P. Verderio and I. Bongarzone. Expression of iron-related proteins differentiate non-cancerous and cancerous breast tumors. *Int. J. Mol. Sci.*, 2017, 18:410-423.
- ¹² L.A. Liotta, V. Espina, A.I. Mehta, V. Calvert, K. Rosenblatt, D. Geho, P.J. Munson, L. Young, J. Wulfkuhle and E.F. Petricoin III. Protein microarrays: Meeting analytical challenges for clinical applications. *Cancer Cell*, 2003, 3:317-325.

- 1
2
3
4 ¹³ L. Yin, Z. Zhang, Y. Liu, Y. Gao and J. Gu. Recent advances in single-cell analysis by mass
5 spectrometry. *Analyst*, 2019, 144:824-845.
6
7 ¹⁴ F. Li, D.W. Armstrong and R.S. Houk. Behavior of bacteria in the inductively coupled plasma:
8 Atomization and production of atomic ions for mass spectrometry. *Anal. Chem.*, 2005,
9 77:1407-1413.
10
11 ¹⁵ K. Shigeta, G. Koellensperger, E. Rampler, H. Traub, L. Rottmann, U. Panne, A. Okinoc and N.
12 Jakubowski. Sample introduction of single selenized yeast cells (*Saccharomyces cerevisiae*) by
13 micro droplet generation into an ICP-sector field mass spectrometer for label-free detection of
14 trace elements. *J. Anal. At. Spectrom.*, 2013, 28:637-645.
15
16 ¹⁶ C.-N. Tsang, K.-S. Ho, H. Sun, W.-T. Chan. Tracking bismuth antiulcer drug uptake in single
17 helicobacter pylori cells. *J. Am. Chem. Soc.*, 2011, 133:7355-7357.
18
19 ¹⁷ Y. Zhou, H. Li and H. Sun. Cytotoxicity of arsenic trioxide in single leukemia cells by time-
20 resolved ICP-MS together with lanthanide tags. *Chem. Commun.*, 2017, 53:2970-2973.
21
22 ¹⁸ M. Corte Rodríguez, R. Álvarez-Fernández García, E. Blanco, J. Bettmer and M. Montes-
23 Bayón. Quantitative evaluation of cisplatin uptake in sensitive and resistant individual cells by
24 single-cell ICP-MS (SC-ICP-MS). *Anal. Chem.*, 2017, 89:11491-11497.
25
26 ¹⁹ L.-N. Zheng, M. Wang, B. Wang, H.-Q. Chen, H. Ouyang, Y.-L. Zhao, Z.-F. Chai and W.-Y. Feng.
27 Determination of quantum dots in single cells by inductively coupled plasma mass
28 spectrometry. *Talanta*, 2013, 116:782-787.
29
30 ²⁰ B. Yang, B. Chen, M. He and B. Hu. Quantum dots labeling strategy for “counting and
31 visualization” of HepG2 cells. *Anal. Chem.*, 2017, 89:1879-1886.
32
33 ²¹ Y. Liang, Q. Liu, Y. Zhou, S. Chen, L. Yang, M. Zhu and Q. Wang. Counting and recognizing
34 single bacterial cells by a lanthanide-encoding inductively coupled plasma mass spectrometric
35 approach. *Anal. Chem.*, 2019, 91:8341-8349.
36
37 ²² L. Mueller, N. Jakubowski, S. Hardt, C. Scheler, P.W. Roos and M. Linscheid. Comparison of
38 different chelates for lanthanide labeling of antibodies and application in a Western blot
39 immunoassay combined with detection by laser ablation (LA-)ICP-MS. *J. Anal. At. Spectrom.*,
40 2012, 27:1311-1320.
41
42 ²³ S. Miyashita, A.S. Groombridge, S. Fujii, A. Minoda, A. Takatsu, A. Hioki, K. Chiba and K. Inagaki.
43 Highly efficient single-cell analysis of microbial cells by time-resolved inductively coupled plasma
44 mass spectrometry. *J. Anal. At. Spectrom.*, 2014, 29:1598-1606.
45
46 ²⁴ G. Han, M.H. Spitzer, S.C. Bendall, W.J. Fantl and G.P. Nolan. Metal-isotope-tagged monoclonal
47 antibodies for high-dimensional mass cytometry. *Nat. Protocols*, 2018, 13:2121-2148.
48
49
50
51
52
53
54
55
56
57
58
59
60

1
2
3
4
5
6
7
8
9
10
11
12
13
14
15
16
17
18
19
20
21
22
23
24
25
26
27
28
29
30
31
32
33
34
35
36
37
38
39
40
41
42
43
44
45
46
47
48
49
50
51
52
53
54
55
56
57
58
59
60

²⁵ X. Lou, G. Zhang, I. Herrera, R. Kinach, O. Ornatsky, V. Baranov, M. Nitz and M.A. Winnik. Polymer-based elemental tags for sensitive bioassays. *Angew. Chem. Int. Ed.*, 2007, 46:6111-6114.

²⁶ T. Konz, E. Añón-Alvarez, M. Montes-Bayon and A. Sanz-Medel. Antibody labeling and elemental mass spectrometry (inductively coupled plasma-mass spectrometry) using isotope dilution for highly sensitive ferritin determination and iron-ferritin ratio measurements. *Anal. Chem.*, 2013, 85:8334-8340.

²⁷ T. Inoue, P.G. Cavanaugh, P.A. Steck, N. Brünner and G.L. Nicolson. Differences in transferrin response and numbers of transferrin receptors in rat and human mammary carcinoma lines of different metastatic potentials. *J. Cell. Physiol.*, 1993, 156:212-217.

²⁸ P.A. Kenny, G.Y. Lee, C.A. Myers, R.M. Neve, J.R. Semeiks, P.T. Spellman, K. Lorenz, E.H. Lee, M. Helen Barcellos-Hoff, O.W. Petersen, J.W. Gray and M.J. Bissell. The morphologies of breast cancer cell lines in three-dimensional assays correlate with their profiles of gene expression. *Mol. Oncol.*, 2007, 1:84-96.

²⁹ H.E. Pace, N.J. Rogers, C. Jarolimek, V.A. Coleman, C.P. Higgins and J.F. Ranville. Determining transport efficiency for the purpose of counting and sizing nanoparticles via single particle inductively coupled plasma mass spectrometry. *Anal. Chem.* 2011, 83, 9361-9369.

³⁰ F. J. Alonso García, D. Turiel Fernández, E. Añón Alvarez, E. Blanco González, M. Montes-Bayón and A. Sanz-Medel. Iron speciation, ferritin concentrations and Fe:ferritin ratios in different malignant breast cancer cell lines: on the search for cancer biomarkers. *Metallomics*, 2016, 8:1090-1096.

³¹ T. Inoue, P.G. Cavanaugh, P. Steck, N. Brunnera and G. Nicolson. Differences in transferrin response and numbers of transferrin receptors in rat and human mammary carcinoma lines of different metastatic potentials. *J. Cell Physiol.* 1993, 156:212-217.

³² D.N. Martin and S.L. Uprichard. Identification of transferrin receptor 1 as a hepatitis C virus entry factor. *Proc. Natl. Acad. Sci.* 2013, 110:10777-10782.

³³ T.R. Daniels-Wells, D.P. Widney, L.S. Leoh, O. Martínez-Maza and M.L. Penichet. Efficacy of an antitransferrin receptor 1 antibody against aidsrelated non-hodgkin lymphoma: a brief communication. *J. Immunother.*, 2015, 38: 307-310.

Tables and Figures

Table 1. Comparison of the results obtained by the commercial ELISA and the modified ELISA using the Nd-labelled antibody and ICP-MS detection.

Table 2. Average number of transferrin receptors per cell (TfR1/cell) obtained by the commercial ELISA and the developed SC-ICP-MS method.

Figure 1. Chromatograms obtained by SEC-UV at 280 nm (A) and SEC-ICP-MS measuring $^{142}\text{Nd}^+$ (B).

Figure 2. Evaluation of the stoichiometry of the labelled antibody by plotting the antigen concentration versus the Nd concentration obtained by ICP-MS.

Figure 3. Box plot of the detected Nd events when identical aliquots of the MDA-MB-231 cells were treated with different concentrations of the Nd-labelled antibody.

Figure 4. Example of cell events obtained detecting Nd by SC-ICP-MS in the (A) MDA-MB-231 and (B) MCF7 cells.

Figure 5. Box plot of the quantitative data obtained representing the number of TfR1 per cell in the two cell models (black trace, MDA-MB-213 and grey trace, MCF7).

Table 1. Comparison of the results obtained by the commercial ELISA and the modified ELISA using the Nd-labelled antibody and ICP-MS detection. Each sample corresponds to three independent replicates.

	Nd-labelled ELISA	Commercial ELISA	Relative differences
Sample	TfR1 (nmol L ⁻¹)	TfR1 (nmol L ⁻¹)	(%)
MDA-MB-231	24 ± 3	22 ± 2	8.3
MCF7	6.1 ± 0.2	5.67 ± 0.02	7.0

Table 2. Average number of transferrin receptors per cell (TfR1/cell) obtained by the commercial ELISA and the developed SC-ICP-MS method.

Samples	TfR1/cell Total (bulk)	TfR1/cell Cell membrane (SC-ICP-MS)	TfR1/cell Intracellular
MDA-MB-231	(1.27 ± 0.01)·10 ⁶	(2.3 ± 0.4)·10 ⁴	(1.25 ± 0.4)·10 ⁶
MCF7	(2.3 ± 0.1)·10 ⁵	(6.4 ± 0.9)·10 ³	(2.2 ± 0.8)·10 ⁵

Figure 1. Chromatograms obtained by SEC-UV at 280 nm (A) and SEC-ICP-MS measuring $^{142}\text{Nd}^+$ (B). A) The blue line corresponds to the original anti-TfR1 antibody (offset: 2 A.U.), the red line correspond to the reduced antibody (offset: 1 A.U.) and the green line corresponds to the labelled antibody containing the MAXPAR[®] chelator and the Nd atoms incorporated. (B) ICP-MS trace of $^{142}\text{Nd}^+$ showing the labelled antibody by SEC-ICP-MS.

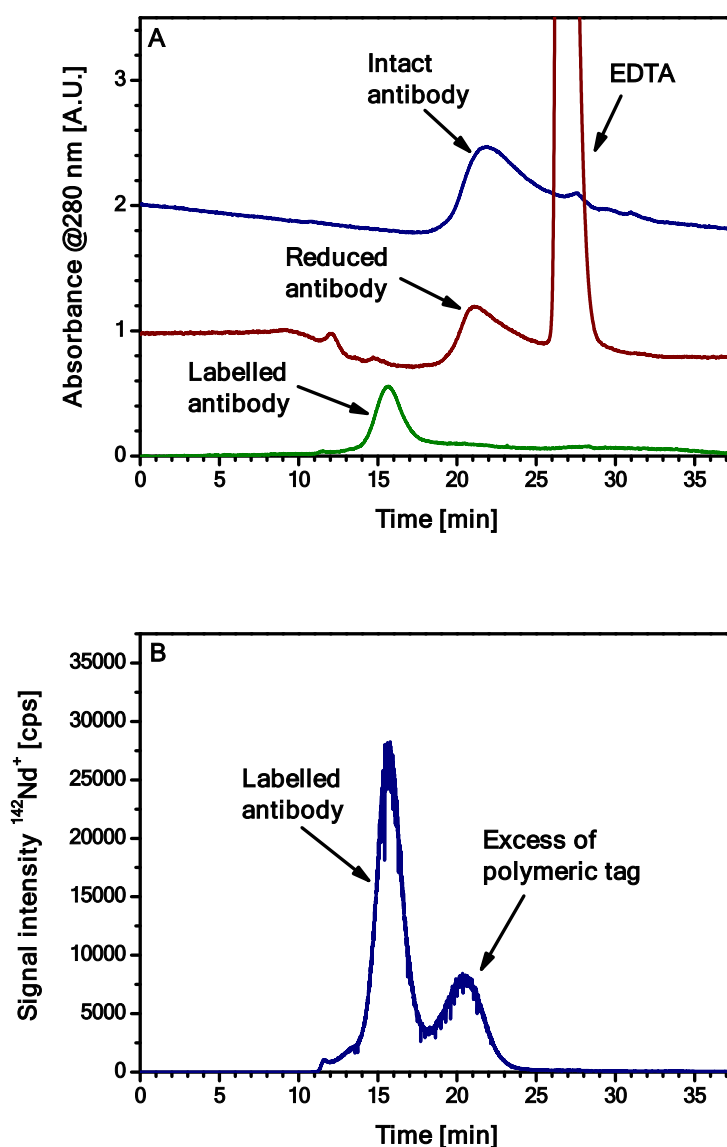


Figure 2. Evaluation of the stoichiometry of the labelled antibody by plotting the antigen concentration versus the Nd concentration obtained by ICP-MS.

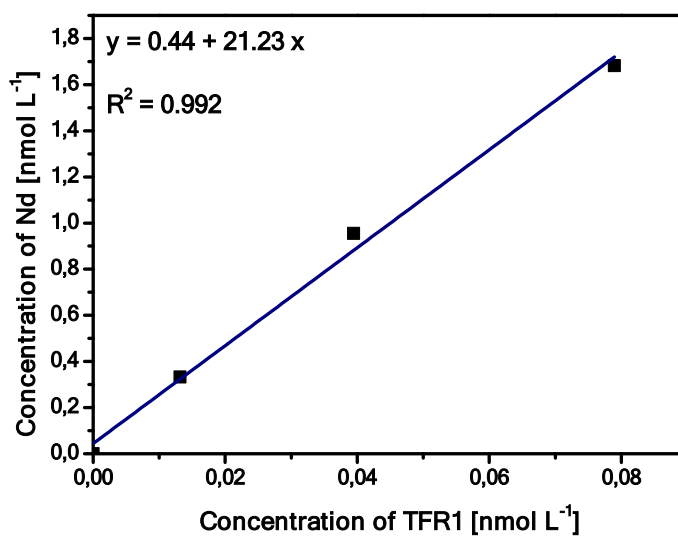


Figure 3. Box plot of the detected Nd events when identical aliquots of the MDA-MB-231 cells were treated with different concentrations of the Nd-labelled antibody.

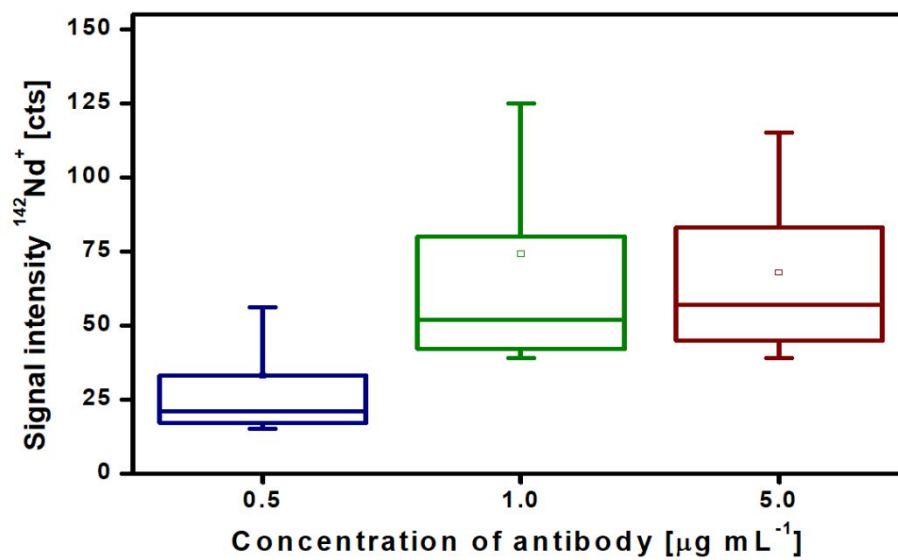


Figure 4. Example of cell events obtained detecting Nd by SC-ICP-MS in the (A) MDA-MB-231 and (B) MCF7 cells.

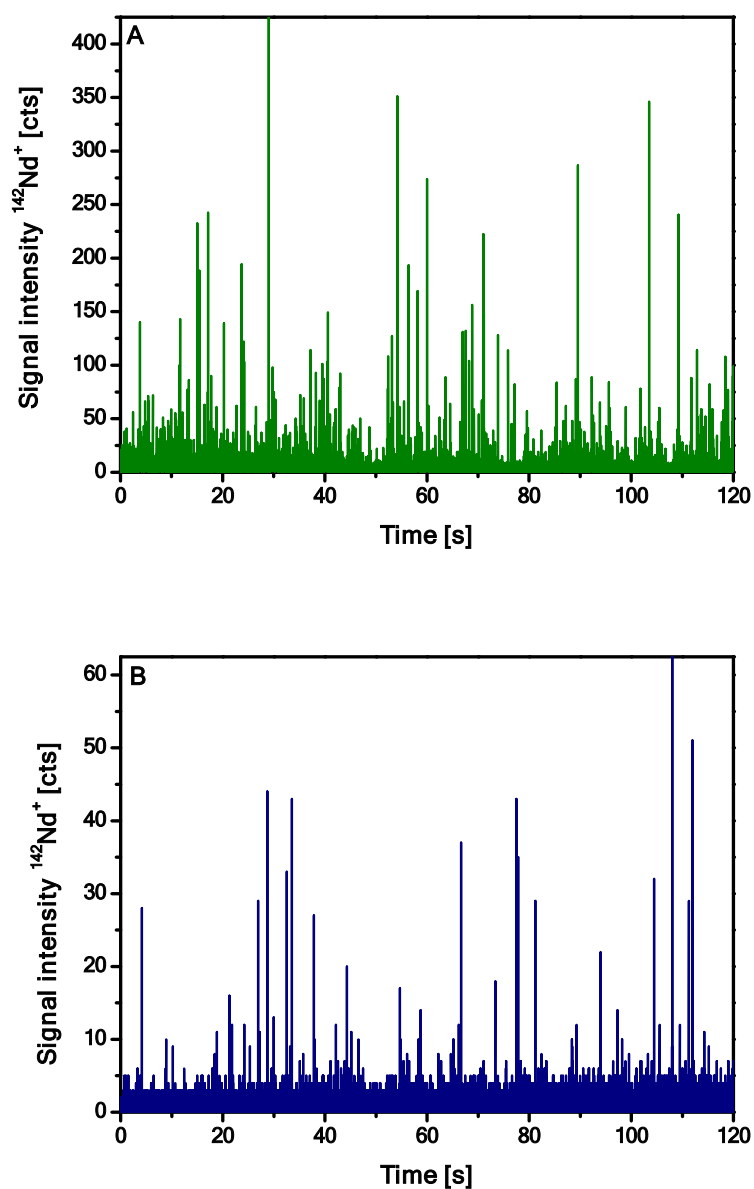


Figure 5. Box plot of the quantitative data obtained representing the number of TfR1 per cell in the two cell models (black trace, MDA-MB-213 and grey trace, MCF7).

